

Assessment of Geothermal Potential of Parts of Middle Benue Trough, North-East Nigeria

Salako, K. A.¹, Adetona, A. A.², Rafiu, A. A.², Alahassan, U. D.², Aliyu, A.² and Adewumi, T.^{3*}

1. Associate Professor, Department of Physics, Faculty of Physical Science, Federal University of Technology, Minna, Nigeria

2. Assistant Professor, Department of Physics, Faculty of Physical Science, Federal University of Technology, Minna, Nigeria

3. M.Sc. Graduated, Department of Physics, Faculty of Science, Federal University, Lafia, Nigeria

(Received: 20 June 2018, Accepted: 14 May 2019)

Abstract

This research deals with assessment of geothermal potential in parts of middle Benue Trough, north-east of Nigeria. The study area lies within the Longitude 9°E – 10°E and Latitude 8°N – 9.50°N with an estimated total area of 18,150 km². Regional/Residual separation was performed on the total magnetic intensity using polynomial fitting. The residual map was divided into 14 overlapping spectral blocks, and the log of spectral energies were plotted against frequency. Centroid depth and depth to top boundary obtained were used to estimate the Curie point depth isotherm, which was then used to compute geothermal heat flow of the study area. The result shows that the geothermal heat flow varies between 50.02 and 85.1 mWm⁻² with highest value in the southern part (Akiri and Ibi) and north-western part (Pankshin) of the area. The geothermal heat flow obtained from this study indicates that the study area possess a good source of geothermal potential. The aero-radiometric data covering the study area was also analysed to estimate the radiometric heat contribution. The analysis of aero-radiometric data shows that the area possesses high content of Uranium, Potassium and Thorium. The radioactive heat production values vary between 1.58 μW/m³ and 2.53 μW/m³ with an average of 2.21 μW/m³. Thus, harnessing the geothermal potential in this area would be of added values and advantage to power generation in Nigeria.

Keywords: Centroid depth, Curie point depth isotherm, Geothermal, Heat flow and Spectral.

1. Introduction

In a contemporary Nigeria where an insufficient production of electricity and other energy sources are operated at lowest ebb, thereby giving rise to an epileptic power supply, poor distribution output and other economic down turn. It is of an ample advantage to locate the potentials of several other forms of renewable energy points including geothermal resources. The availability of geothermal energy, which results from radioactive decay of minerals within Earth's core are readily utilised by several country of the world. However, in Nigeria quite a little of this alternative energy sources are known. This is even with the existence of the following known potential entities such as; Ikogosi warm spring (37 °c) in Ekiti State, Wikki warm spring (39 °c) in Bauchi State, and Rafin-Ruwa warm spring (45 °c) located in Plateau State (Babalola, 2004; Sedara and Joshua, 2013; Ikechukwu et al., 2015).

Geothermal energy is a viable and sustainable source of energy from deep inside the earth (Dickson and Fanelli, 2004) that has the potential of supplying source base-load, drive long-term energy and emission reduction of greenhouse gas (Muffler and Cataldi, 1978). It is viewed as a sustainable power source asset from the ground, as the heat exuding from the inside of the Earth is basically inexhaustible. The Earth interior can be relied upon to remain greatly hot for billions of years to come, guaranteeing a basically inexhaustible stream of heat.

The middle Benue Trough has received limited attention in the past from earth scientists partly due to the lack of immediate geologic and economic values. However, in view of increased efforts to explore for new and more energy locations in Nigeria, it is fast becoming an important study area (Ajayi and Ajakaiye, 1986;

*Corresponding author:

tydon4real@yahoo.co.uk

Akande et al., 2011; Bako, 2010; Kasidi and Nur, 2012; Nwosu, 2014; Offodile, 1976; Ofoegbu, 1985; Onuoha et al., 1994). Since geophysical crustal temperature studies in the area are minimal, the results of this study would definitely add to the available geophysical informations in that like.

1-1. Location and Geology of the Study Area

The study area (Fig. 1) is located in the north-eastern part of Nigeria, lying between Latitudes 8°N and 9.5°N and longitudes 9°E and 10°E with estimated total area of 18,150 km². It is bounded by middle Benue Trough (Fig. 2). The Benue Trough comprises of a progression of rift basins that model a portion of the Central West African Rift System of the Niger, Cameroon, Chad and Benin Basement fracture, subsidence, block faulting and cracking.

Benkhelil (1982 and 1989), pointed out that the Benue Trough generally has been geographically and structurally subdivided into three parts erroneously termed as "lower Benue Trough", "middle Benue Trough" and an "upper Benue Trough". The area is housed by middle Benue trough, the study conducted by Offodile (1976) distinguishes six sedimentary formations in the middle Benue Trough, which are Asu River Group, Keana Formation, Awe Formation, Ezeaku Formation, Awgu Formation and Lafia Formation.

The oldest, Asu River Formation being middle to Albian and the youngest, Lafia Formation is of the Maestrichtian age. The lithologic composition of the Asu River Group comprises limestones, shales, micaceous siltstones, mudstones and clays (Offodile, 1976; Obaje, 1994).

The deposition of the Awgu Formation marks the end of marine sedimentation in this part of the Benue Trough. The formation is made up of bluish-grey to dark-black carbonaceous shale, calcareous shale, shaley limestones, limestones, sandstones, siltstones, and coal seams (Offodile, 1976).

The deposition of the Ezeaku Formation is attributed to the beginning of marine

transgression in the Late Cenomanian. The sediments are made up mainly of calcareous shales, micaceous fine to medium friable sandstones and beds of limestones which are in places shelly.

The Awe Formation was deposited as passage (transitional) beds during the late Albian to early Cenomanian regression. The formation consists of flaggy, whitish, medium to coarse grained calcareous sandstones, carbonaceous shales and clays.

The Keana Formation resulted from the Cenomanian regression that deposited fluvio-deltaic sediments. The formation consists of cross-bedded, coarse grained feldspathic sandstones, occasional conglomerates, and bands of shales and limestones towards the top (Obaje, 1994).

The Lafia Formation is the youngest formation in this area. The formation was deposited under continental condition (fluvial) in the Maastrichtian and lies unconformably on the Awgu Formation. It is lithologically characterized by ferruginized sandstones, red, loose sands, flaggy mudstones, clays and claystones (Obaje, 1994).

The work of Cratchley and Jones (1965), Burke et al. (1970), Offodile (1976 and 1984), Osazuwa et al. (1981), Ofoegbu (1985) and Patrick et al. (2013) have more on the geology of the Benue Trough.

2. Materials and Method

For this research, six aeromagnetic data sheet and six aero-radiometric data sheet used were procured from the Nigerian Geological Survey Agency (NGSA), Abuja as part of across the nation aeromagnetic and aero-radiometric study carried out in 2009 by Fugro Airborne survey. The six aeromagnetic and aero-radiometric data sheets used were 190 (Pankshin), 191 (Wasa), 211 (Kwalla), 212 (Shendam), 232 (Akiri), 233 (Ibi), which correspond to latitudes 8°N to 9.5°N and longitudes 9°E to 10°E. Each gridded map scaled 1:100,000 covers an area of about 3025 km² (i.e. 55 km x 55 km) while the total area investigated covers 18,150 km².

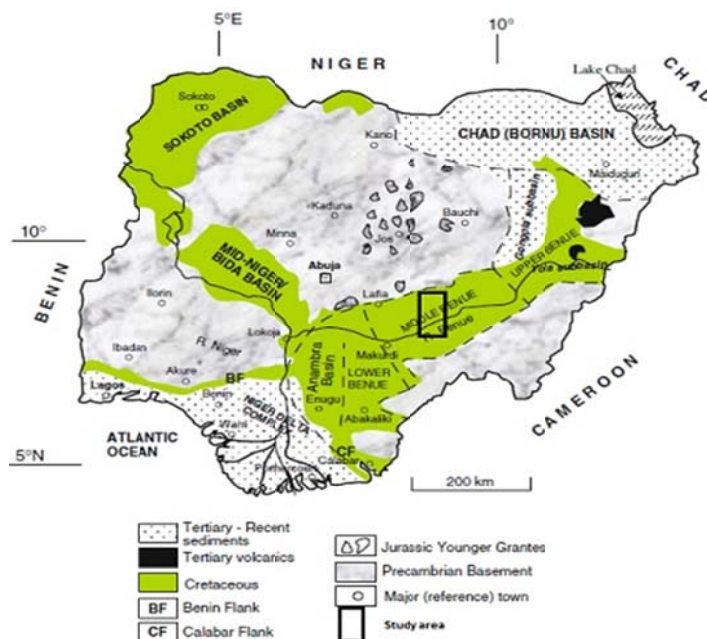


Figure 1. Geological Map of Nigeria showing the study area in black outlined (Modified after Obaje, 2009).

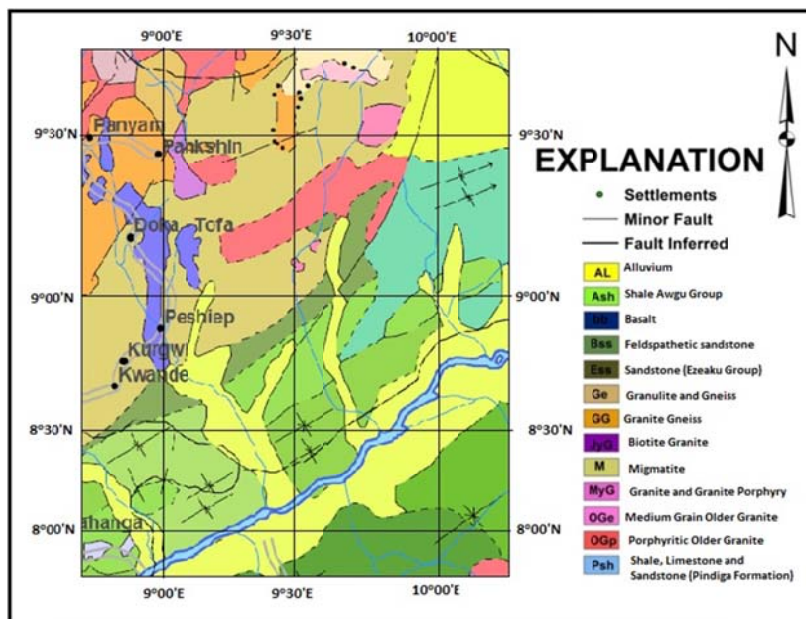


Figure 2. Geological map of the middle Benue Trough (Extracted from Geological Map of Nigeria, NGS (2006)).

2-1. Spectral method

It is a depth estimating method pioneered by Bhattacharyya (1966) and later developed by Spector and Grant (1970). It has been utilized widely in the analysis of magnetic anomalies in the determination of average depth to the top of magnetic basement, computation of crustal thickness and thermal framework of the earth (Bhattacharyya and Leu, 1975; Cornad et al., 1983, Onuoha et al.,

1994; Nwogbo, 1997; Eleta and Udensi, 2012; Salako and Udensi, 2013; Mishra and Naidu, 1974; Kasidi and Nur, 2013; Shuey et al., 1977; Tanaka et al., 1999). The techniques permits an estimate of depth of magnetized blocks of varying depth, width, thickness and magnetisation. Most approaches used include Fourier transformation of the aeromagnetic data to estimate the energy (or amplitude) spectrum

by transforming the spatial data into frequency domain.

Spector and Grant (1970) illustrated that the thickness depth and width of a magnetic source ensemble could affect the shape of energy spectrum. The strong term that shapes this energy spectrum is the depth factor. They demonstrated that the depth could be estimated using Equation (1).

$$E(r) = e^{-2Zr} \quad (1)$$

where $E(r)$ = spectral energy Normalised

r = frequency

h = depth

If h is the mean depth of a layer and the depth factor for the ensemble of anomalies is e^{-2rh} ; hence, a plot of the energy spectrum of a single ensemble of prism against angular frequency r would yield a straight line graph whose slope is directly proportional to the average source depth, h of that ensemble (Spector and Grant, 1970). That is, the logarithm plot of the radial frequency would yield a straight line whose slope is:

$$m = -2h$$

$$h = -\frac{m}{2} \quad (2)$$

Equation (2) can be specifically applied if the frequency unit is in radian per unit distance (kilometer as it is in this research), if its unit is in cycle per unit distance as it is in this work, the expression becomes:

$$h = -\frac{m}{4\pi} \quad (3)$$

From the slopes of the plot, the first and the second magnetic source depth was respectively estimated.

2-2. Curie point depth estimation

The bottom of a magnetic source indicate the thermal boundary at which magnetic mineral in the crust move from ferromagnetic status to paramagnetics as a result of the increase in temperature as depth increases down the crust (Nagata, 1961; Ross et al., 2006). This thermal boundary is referred to as Curie point depth and it is the nethermost part of the crust to have material which develops discernible mark in a magnetic anomaly map (Bhattacharyya and Leu, 1975). This point is assumed to be the depth for the geothermal source (magmatic chamber), where most geothermal reservoir tapped their heat from a

geothermal environment (Eleta and Udensi, 2012).

This Curie point has a temperature of $550 \text{ }^\circ\text{C} \pm 30 \text{ }^\circ\text{C}$. For temperature above Curie-point, magnetic materials lose their magnetic ordering and both induced and remnant magnetisation disappear, thus for temperatures above 580°C , those materials will begin to encounter ductile deformation.

The methods of Curie Point Depth determination utilize spectrum analysis techniques to separate influences of the different body parameters in the observed magnetic anomaly field. Fundamentally, the method of Spector and Grant (1970) estimates the average depth to the top boundary of the magnetized layer from the slope of the log power spectrum while the method of Bhattacharyya and Leu (1975) obtains the depth to the centroid (effects from the bottom) of the causative body using a single anomaly interpretation. Okubo et al. (1985) effectively combined and expanded both methods to propose an algorithm for regional geomagnetic interpretation oriented to the purposes of geothermal exploration.

The Curie point depth is evaluated in two stages as proposed by Bhattacharyya and Leu (1975); the first stage is the estimation of depth to centroid Z_0 of magnetic source from the slope of the longest wavelength part of the spectrum, using Equation (4) (Okubo et al., 1985 and 1989; Dolmaz et al., 2005; Eleta and Udensi, 2012).

$$\ln\left[\frac{\sqrt{p(s)}}{|s|}\right] = \ln A - 2\pi|s|Z_0 \quad (4)$$

where

$P(s)$ = radially averaged power spectrum of the anomaly,

$|s|$ = the wave number,

and A = constant.

The second stage is the estimation of the depth to the top boundary Z_1 from the slope of the second longest wavelength part of the spectrum (Okubo et al, 1985 and 1989; Dolmaz et al. 2005; Eleta and Udensi, 2012):

$$\ln\sqrt{p(s)} = \ln B - 2\pi|s|Z_1 \quad (5)$$

where B , is the sum of constant independent of $|s|$.

The basal depth Z_b also known as Curie point depth was calculated from Equation (6).

(Okubo et al., 1985 and 1989; Eletta and Udensi, 2012).

$$Z_b = 2Z_0 - Z_t \quad (6)$$

where Z_0 is centroid depth and Z_t is depth to the top boundary.

2-3. Geothermal Gradient and Heat Flow

The fundamental relation for conductive heat movement is Fourier's law (Tanaka et al., 1999). In one-dimensional case under the notions that the direction of the temperature change is vertical and the temperature gradient ($\frac{dT}{dz}$) is constant, Fourier's law is expressed as given in Equation (7) (Tanaka et al., 1999; Kasidi and Nur, 2012; Ofor and Udensi, 2014):

$$q = -k \frac{dT}{dz} \quad (7)$$

where

q = the heat flux (heat transfer per unit time)

k = coefficient of thermal conductivity.

From Tanaka et al. (1999), the Curie temperature (θ) can then be estimated from the expression:

$$\theta = \left(\frac{dT}{dz}\right)Z_b \quad \text{and} \quad \frac{dT}{dz} = \left(\frac{\theta}{Z_b}\right) \quad (8)$$

making $\frac{dT}{dz}$ (Geothermal gradient) the subject of the formula in Equations (7) and (8) and comparing the result will give:

$$Z_b = \theta \frac{k}{q} \quad (9)$$

Equation (9) shows that Curie point depth is inversely proportional to heat flow and signifies that areas of high heat flow experience shallower Curie point depth, on the other hands, those with relatively low heat flow have deeper Curie point depth (Tanaka et al., 1999; Ross et al., 2006). An average surface heat flow value was estimated using Equations (7) and (8) and was predicated on possible Curie temperature of 580°C and thermal conductivity of 2.5 $\text{Wm}^{-1}\text{C}^{-1}$ as suggested by Stacey (1977), which is the average thermal conductivity for igneous rocks.

2-4. Airborne Radiometric Method

Geophysical survey is appreciated more when two or more geophysical methods are employed. Generally airborne radiometric

survey that includes the repeated radiometric measurement of gamma ray flux that strikes at least one detector mounted in a moving grid like pattern aircraft, is always flown in conjunction with the magnetic method.

Most of the continental heat flow emanates from the decay of radioactive isotopes in the crust; therefore, locating regions having higher concentration of radioactive isotope or estimating the radioactive heat production can be the same as locating areas with high heat flow (Holmberg et al., 2012).

2-5. Radioactive Heat Analysis

More than 98% of present-day heat production is the result of the decay series ^{238}U and ^{232}Th and the single step decay of ^{40}K . The isotope ^{235}U has a significantly shorter half-life than ^{238}U . Other short-lived radioactive isotopes may have made significant thermal contributions in early stages of the Earth's history, but they are not detectable now. Other long-lived radioactive isotopes also exist, but their decay rates are so slow that they have never made any significant contribution to the Earth's heat (Slagstad, 2008).

Thus, According to Kuforijimi and Christopher (2017), Megwara et al. (2013), Holmberg et al. (2012) and Abraham et al. (2014); radiogenic heat production (H) is primarily concerned with the decaying of radioactive isotopes of ^{232}Th , ^{238}U and ^{40}K and can be computed in accordance with the concentration (C) of the respective elements via empirical equation by Rybach (1976):

$$H(\mu\text{W}/\text{m}^3) = \rho(9.52 C_U + 2.56 C_{Th} + 3.48 C_K) \times 10^{-2} \quad (10)$$

where,

H = radioactive heat production

ρ = density of rock adapted from Kuforijimi and Christofer (2017) and Telford et al. (1990).

C_u , C_{Th} and C_k are the concentrations of Uranium, Thorium and Potassium respectively.

3. Result and Discussion

3-1. Total magnetic intensity anomaly and the residual magnetic intensity anomaly

The total magnetic intensity map, TMI (Fig. 3), and the residual magnetic intensity

map (Fig. 4) show variation of highs and lows in magnetic signature. About one third of the map can be seen to be greenish, which may correspond to alluvium deposition in the southern part of the study area, the pink colouration depicts high magnetic signature while blue depicts low magnetic signature and yellow indicates intermediary magnetic features.

The negative values imply areas that are magnetically subdued or quiet while the positive values are magnetically responsive. The magnetically subdued areas are the magnetic lows of the study area and this is typical of a sedimentary terrain while the magnetic responsive areas are the magnetic highs regions, which are assumed to be due to the likely presence of outcrops of crystalline igneous or metamorphic rocks, deep seated volcanic rocks or even crustal boundaries. From Fig. 3, the high magnetic anomaly, which can probably be attributed to igneous intrusion and shallower sediment is well pronounced in the central part, trending approximately east-west similar to the one in residual map (Fig. 4). The high magnetic

signature can also be found in the north-eastern part trending north-west while the low magnetic anomalies associated with the sedimentary region was well pronounced in north-western, north-eastern, while other scattered at the edges of north-eastern part of the study area. The low magnetic signature is well pronounced in the northern part of the study area, though few others could also be found at southern part of the study area trending NE-SW.

The varying amplitude of these magnetic anomalies is an indication of different sedimentary thickness in the study area. These variations in the anomaly amplitude may also indicate possibly the occurrences of basement complex rocks containing varying amounts of magnetic minerals. The traced line on the map is probably a fracture (fault line). At some places on the southern part of the residual map (Fig. 4), there is a break in the NE-SW trending magnetic low present on the total magnetic map (Fig. 3). These anomalies may be due to the magnetic source of shallow origin.

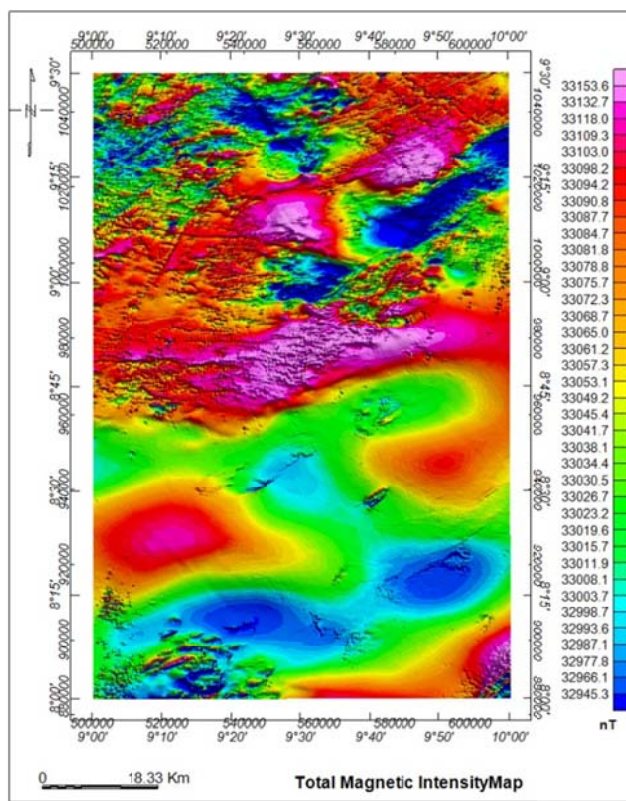


Figure 3. Total Magnetic Intensity map of the study area.

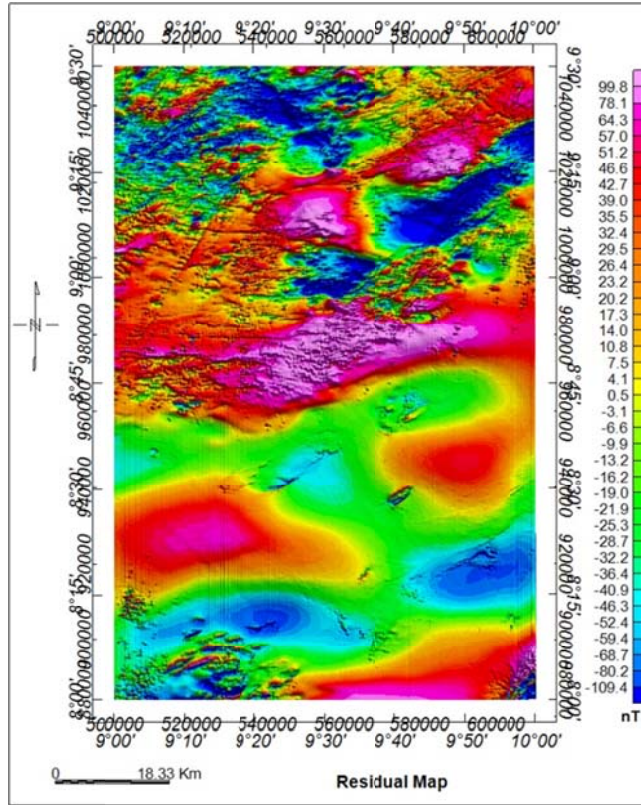


Figure 4. Residual map of the study area.

3-2. Spectral analysis

The residual map (Fig. 4) of the study area was divided into 14 (Blocks A - N) overlapping magnetic sections in which six (Blocks A - F) covered 55 km by 55 km data points, three other division (Block G, H and I) covered 110 km by 55 km data points, J, K and L covered 110 km by 110 km and Block M and N covered the remaining 165 km by 55 km part of the study area. The divisions of

residual map into spectral sections of blocks were done with Oasis Montaj. The analysis was carried out using a spectral program plot (SPP) developed with MATLAB. Fig. 5 is the Graph of the logarithm of spectral energies against frequencies obtained for blocks A and B. The estimated value for centroid depth and depth to the top boundary, Z_0 and Z_t respectively were detailed in Table 1.

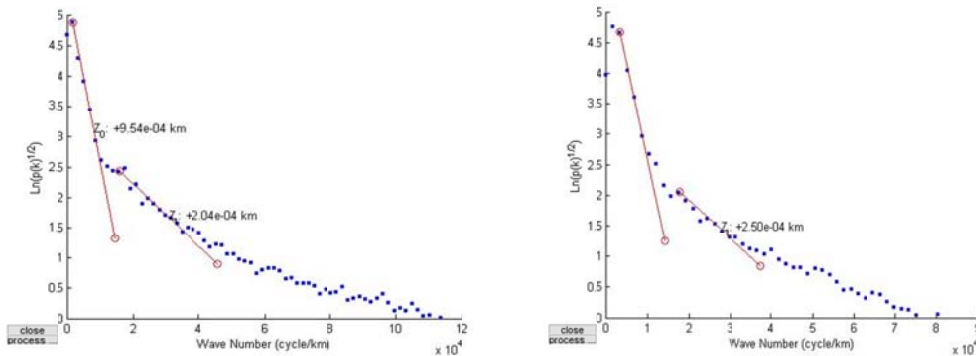


Figure 5. Graph of the logarithm of spectral energies against frequencies obtained for block A and B.

Table 1. Location and depth estimation of centroid depth (Z_0), depth to basement (Z_i), CPD (Z_b), geothermal gradient and Heat flow.

Blocks	Longitude (degree)	Latitude (degree)	Depth to centroid, Z_0 (km)	Depth to the top boundary Z_i (km)	Curie point depth, Z_b (km)	Geothermal gradient ($^{\circ}$ C/km)	Heat flow (mW/m^2)
A	9.25	9.25	9.54	2.04	17.04	34.04	85.1
B	9.75	9.25	13.30	2.50	24.1	24.06	60.17
C	9.25	8.75	11.40	2.40	20.66	28.07	70.19
D	9.75	8.75	10.82	1.98	19.66	29.50	73.75
E	9.25	8.25	9.56	1.20	17.92	32.48	81.194
F	9.75	8.25	9.36	1.40	17.32	33.49	83.71
G	9.5	9.25	10.60	2.00	19.20	30.21	75.52
H	9.5	8.75	15.40	3.20	27.40	21.17	52.92
I	9.5	8.25	10.44	1.70	19.18	30.24	75.59
J	9.5	9.0	11.04	1.50	20.58	28.18	70.45
K	9.5	8.0	12.98	1.84	24.12	24.05	60.11
L	9.25	8.25	14.70	2.08	27.32	21.23	53.07
M	9.75	8.25	11.32	1.86	20.78	27.91	55.82
N	9.5	8.25	12.42	1.65	23.19	25.01	50.02

3-3. Curie point Depth (CPD)

The results of the spectral analysis of aeromagnetic anomalies over the area shows that the Curie point depth estimates (using equation 6) range between 17.04 km and 27.4 km (Table 1). Literatures such as (Bhattacharyya and Leu, 1975; Cornad et al., 1983, Tanaka et al., 1999; Nwankwo et al., 2011; Eleta and Udensi, 2012) indicate that CPD is greatly dependent on the geologic conditions of an area under consideration, the CPD are shallower in volcanic and geothermal fields.

Fig. 6 is the Curie point depth contour map. High values of 21 km to 27.5 km could be seen at the central region (Kwalla and Shendam) to the north-eastern part (Wasa) and lower values of 17 km to 19.5 km could be observed at the central southern part (Akiri and Ibi) and the north western part (Pankshin). The low value might be as a result of igneous intrusion or as a result of the dominance of Ezeaku formation (sandstone and limestone) in the area.

3-4. Geothermal Gradient

Using a Curie temperature of 580 $^{\circ}$ C and the

estimated Curie point depths, geothermal gradient variation were computed and the geothermal gradient map (Fig. 7) was plotted. The results show that geothermal gradients (Table 1) vary between 21.17 $^{\circ}$ C/km and 34.04 $^{\circ}$ C/km with average value of 27.83 $^{\circ}$ C/km. Most of the higher values are located at the southern and north-western parts of the study area.

3-5. Heat Flow

The results (Table 1) show that the heat flow values (estimated in accordance with equation 7) of the area vary between 50.02 mW/m^2 and 85.1 mW/m^2 , and the heat flow contours are plotted in Fig. 8. The contour shows low values of 52 mW/m^2 to 70 mW/m^2 , which could be observed at the central region (Kwalla and Shendam) to the north-eastern part (Wasa) and higher value of 74 mW/m^2 to 85 mW/m^2 can be located at most part of the southern area (Akiri and Ibi) and the north western part (Pankshin). The higher value might be as a result of the dominance of Ezeaku formation (sandstone and limestone) in the area. Both Geothermal gradient and heat flow show a linear

relationship in their lineament (both in locations and trend) as areas of high heat flow correspond to high geothermal gradient and vice versa and both also show an inverse relationship to Curie point depth as projected

by Equations (7), (8) and (9). This result along with the Curie point depth agreed favourably with Kasidi and Nur (2012 and 2013) who worked on the eastern part of the study area.

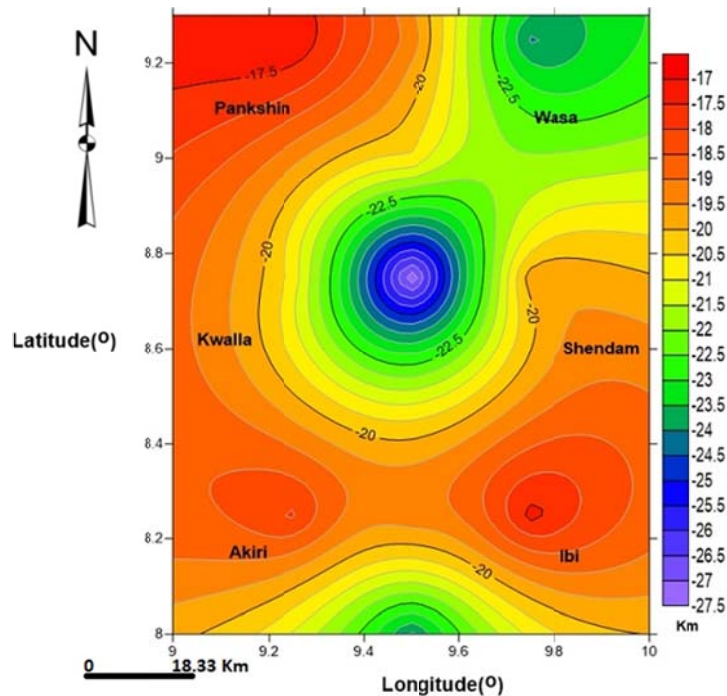


Figure 6. Curie point depth contour map.

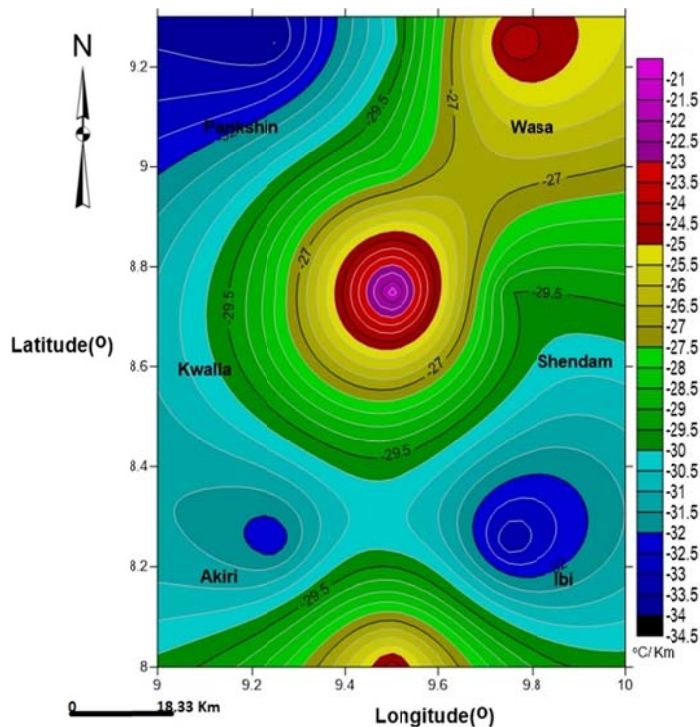


Figure 7. geothermal gradient contour map.

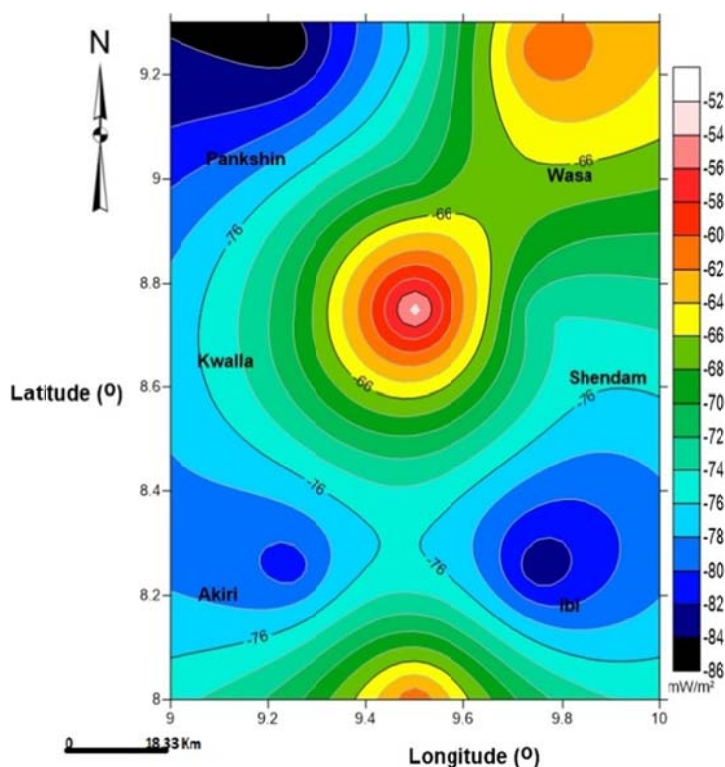


Figure 8. contour map of the heat flow anomaly contour interval is 2 km.

3-6. Radiometric data analysis

3-6-1. Potassium (K) content map of the study area

The K concentration map (Fig. 9) shows high concentration of K around Pankshin and Wamba, it shows low concentration value in the region around Kwalla, Ibi and part of Akwana.

3-6-2. Thorium (Th) content map of the study area

The Th concentration map (Fig. 10) shows high concentration of Th in most part of the area; however, the concentration was not evenly distributed. Higher concentration values can be observed in the southern (Ibi and Akwana) and eastern-central (Kwalla). The north-western (Wase) region were mostly dominated by the highest observed concentration value. Low value were found in part of the west-central and at the edge of south-eastern part, the higher value obtained in the region around Ibi and Akwana may be

as a result of high shales, sandstone and limestone content associated with Ezeaku (Ibi and Kwalla) Formation and Asu River Group (in Akwana) as indicated in the geological map (Fig 2) of the area (Obaje, 1994).

3-6-3. Uranium (U) content map of the study area

From the Uranium concentration map (Fig. 11), values between 1.68 ppm to 6.08 ppm for Uranium concentration were observed in the whole of the study area. It shows that though unevenly distribution of relatively higher concentration of Uranium can be observed through most part of the area, the highest values were predominant in the north-western (Wase) and east-central (Kwalla) to the south-western (Ibi) region ranging from 4.50 ppm to 6.08 ppm, this high concentration value in Ibi, Kwalla and part of Akwana may be attributed to high content of shales and limestone in those areas.

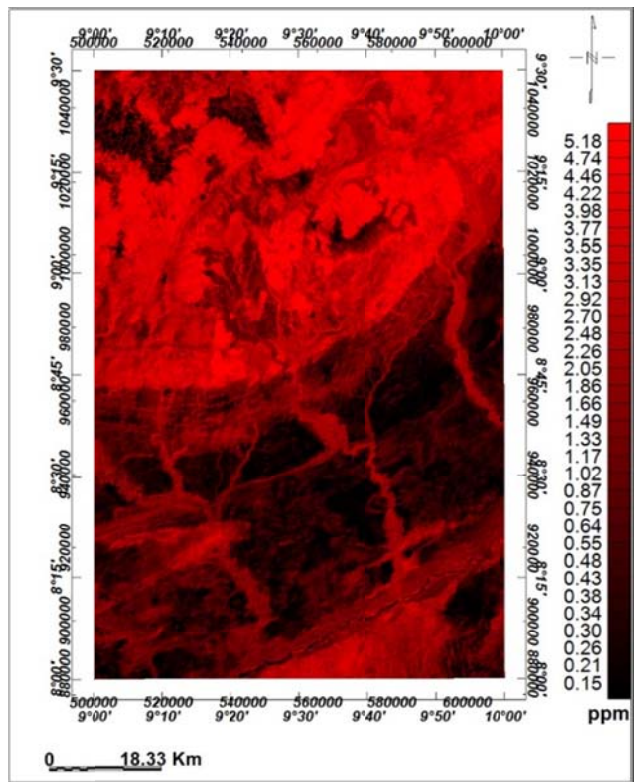


Figure 9. K-content map of the study area.

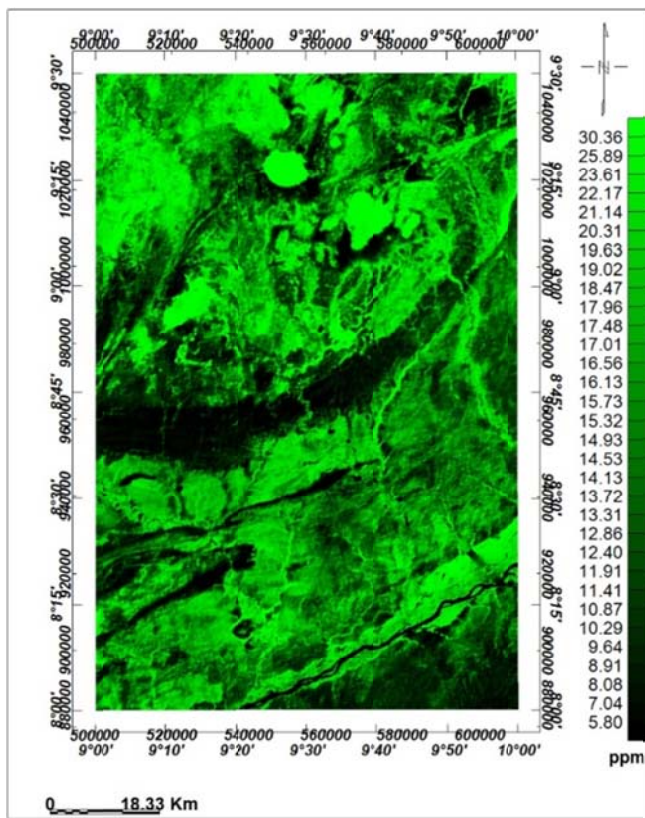


Figure 10. Th-content map of the study area.

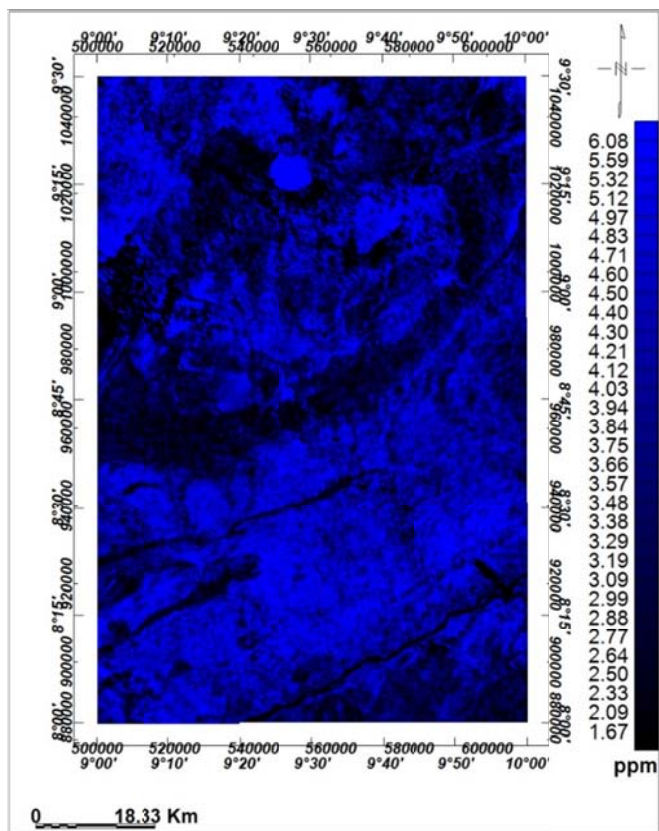


Figure 11. U-content map of the study area.

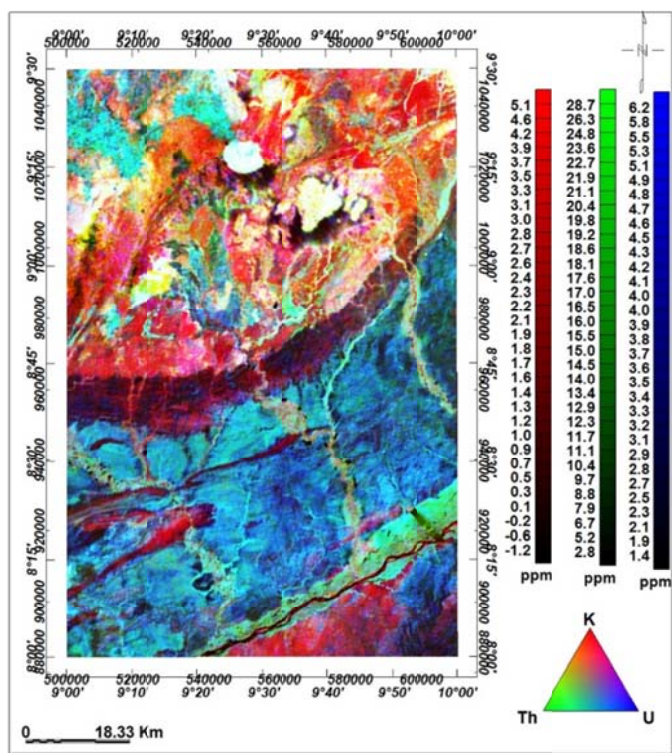


Figure 12. Ternary map of the study area.

3-6-4. Ternary (K, Th, U) content map of the study area

The ternary map (Fig. 12) of the area was generated from the combination of uranium, thorium and potassium concentrations, it depicts the concentration of K (in red), Th (in green) and U (in blue), the white colour is related with high counts of the three isotopes, while the black colour depicts low levels of the three isotopes.

It was noticed that potassium concentration was high in most part of the northern region trending from west-central to the north-eastern part, higher values of potassium concentration were also observed in the south-eastern edge of the area, which could be attributed to high concentration of magnetite gneiss in Wase and part of Pankshin area as indicated in the geological map (Fig. 2). The thorium and uranium concentration are well pronounced from south-western to the east-central region. This higher value of both thorium and uranium concentrations could be as a result of shale, sandstone and limestone. The uranium and thorium concentration shows an approximately linear relationship with heat flow anomaly both in trend and location, thus, they are great contributor to the high heat flow value obtained in Ibi and Kwalla areas of the study area.

3-6-5. Radiogenic Heat Production (RHP)

The potassium, thorium and uranium content maps of the study area were tied alongside

with the Total Magnetic Intensity map. Five profiles (Fig. 13) running SW-NE with the exception of profile 5, which runs NW-SE. Average concentration of each isotope along each profile were computed.

The following eight rock units: Alluvium, Eze Aku Formation, Awgu Ndeaboh Formation, Asu River Group, pan Africa Younger granitoids, pan Africa Older granitoids, magnetite gneiss, basalt were identified in the geological map (Fig. 2) of the area. Their average specific gravity or density alongside with average concentration of each isotope along each profile were applied for further calculation of the radiogenic heat production. RHP (Table 2) values for each profile were calculated based on Equation (10) with an average value of $2.2 \mu\text{W}/\text{m}^3$. This value is greater than the average heat production of the Precambrian shield, $0.77 \pm 0.08 \mu\text{W}/\text{m}^3$ given by Jaupart and Mareschal (2003). Although they indicated that on a local scale, the variation from their value could be significant. In the present study, the difference in the area RHP may be attributed to the high radioelement contents found in the area.

From the result (Table 2), it shows that lowest average RHP were obtained in profiles 2 and 3 that majorly run through the region with high magnetic signature (Fig. 1) and low heat flow (Fig. 13) while profiles 1 and 4 run through the region with low magnetic signatures (Fig. 1) and where the heat flow (Fig. 13) values are highest.

Table 2. Summary of the result for radioactive heat analysis.

Isotopes	C_K (ppm)	C_{Th} (ppm)	C_U (ppm)	RHP ($\mu\text{W}/\text{m}^3$)
Profile 1	3.83	19.68	3.81	2.53
Profile 2	2.98	15.27	3.55	1.58
Profile 3	0.73	14.80	4.38	2.08
Profile 4	0.86	17.20	4.22	2.21
Profile 5	1.66	17.13	3.94	2.20

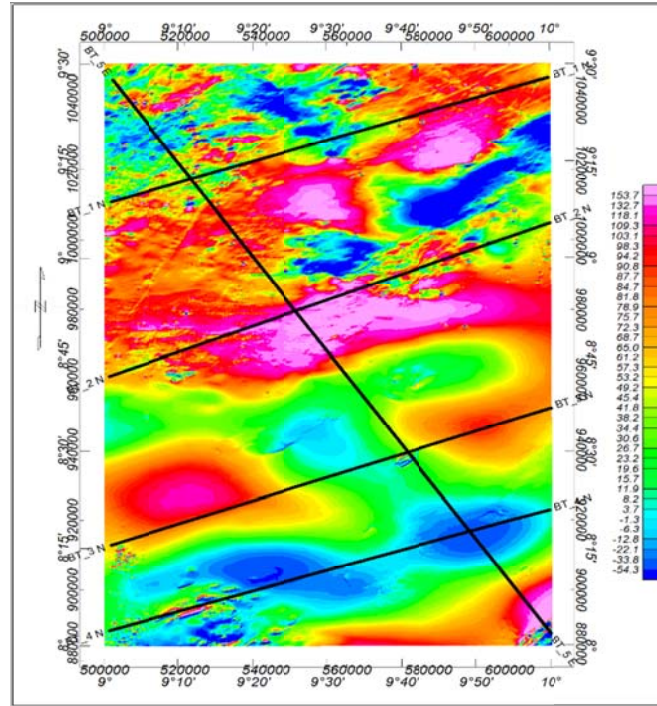


Figure 13. Total Magnetic Intensity Map showing radiometric models drawn.

4. Conclusions

In this study, spectral method was used to analyse aeromagnetic data to differentiate the frequency characteristics between the magnetic effects from the top and bottom of the magnetised layer in the crust to estimate the Curie point depth in the study area. It is found out that the region is characterized by shallow Curie depths of 17.04 km and 27.4 km and high heat flow of 50.02 mWm^{-2} and 85.1 mWm^{-2} . Based on the previous research works (Kasidi and Nur, 2012 and 2013), this value obtained from the study indicates that the study area (especially Ibi, Akiri and Wasa regions) have the highest heat flow and possess a great source of geothermal potential. However, the authors were constrained by the lack of supplementary information (like borehole log) or other data about temperature measurements at depth, which would have been used to compare the heat flow result with the radioactive heat production (RHP) value expected in Precambrian Basement Complex. It is found out that the RHP of the area varies between 1.58 and $2.53 \mu\text{W/m}^3$.

References

Abraham, E. M., Lawal, K. M., Ekwe, A. C.,

Alile, O., Murana, K. A. and Lawal, A.A., 2014, Spectral analysis of aeromagnetic data for geothermal energy investigation of Ikogosi Warm Spring-Ekiti State, southwestern Nigeria. *Geothermal Energy*. 2(1), 1, doi:10.1186/s40517-014-0018-9.

Ajayi, C. O. and D. E. Ajakaiye, 1986, Structures deduced from gravity data in the middle Benue, Nigeria. *Journal of African Earth Sciences*, 5, 359-369.

Akande, S. O., Egenhoff, S. O., Obaje, N. G. and Erdtmann, B. D., 2011, Stratigraphic evolution and petroleum potential of middle cretaceous sediments in the lower and middle BenueTrough, Nigeria: Insights from New Source Rock Facies Evaluation. *Petroleum Technology Development Journal* (ISSN 1595-9104).

Babalola, O. O., 2004, High-Potential geothermal energy resources areas of Nigeria and their geological and geophysical assessment. *American Association of Petroleum Geologists Bulletin*, 1, 68, 4, AAPG.

Bako A. S. J., 2010, Geothermal energy potential in the part of middle benue trough located in Nasarawa state. A thesis submitted to the postgraduate school,

- Ahmadu Bello university, Zaria, Nigeria.
- Benkhelil, J., 1982, Benue Trough and Benue Chain. *Geological Magazine*, 119, 155-168.
- Benkhelil, J., 1989, The origin and evolution of the cretaceous Benue Trough (Nigeria). *Journal of African Earth Sciences*, 8, 251-282.
- Bhattacharyya, B. K., 1966, Continuous spectrum of the total magnetic field anomaly due to a rectangular prismatic body. *Geophysics*, 31, 97-121.
- Bhattacharyya, B. K. and Leu, L. K., 1975, Analysis of magnetic anomalies over Yellowstone National Park: mapping of Curie point isothermal surface for geothermal reconnaissance. *Journal of Geophysical Research*, 80, 4461-4465.
- Burke, K. C., Dessauvage, T. F. J. and Whiteman, A. J., 1970, Geologic history of the Benue Valley and adjacent areas. In: Dessauvage T.F.J. and Whiteman, A.J. (eds): *African Geology*, University of Ibadan Press, Nigeria, 187-206.
- Connard, G., Couch, R. and Gemperle, M., 1983, Analysis of Aeromagnetic measurements from the Cascade Range in Central Oregon. *Geophysics*, 48, 376-390.
- Cratchley, C. R. and G. P. Jones, 1965, An interpretation of the geology and gravity anomalies of the Benue Valley, Nigeria. *Journal of Geology and Geophysics*, 1, 1-26.
- Dickson, M. and Fanelli, M., 2004, What is geothermal energy. *Instituto di Geoscienze e Georisorse, CNR*, Pisa, Italy.
- Dolmaz, M. N., Ustaomer, T., Hisarli, Z. M. and Orbay, N., 2005, Curie point depth variations to infer thermal structure of the crust at the African-Eurasian convergence zone, SW Turkey. *Earth Planets Space*, 57, 373-383.
- Eletta, B. E. and Udensi, E. E., 2012, Investigation of Curie point isotherm from the magnetic field of Easter sector of central Nigeria. *Global Journal of Geosciences*, 2(4), 101-106.
- Holmberg, H., Naess, E. and Evensen, J. E., 2012, Thermal Modeling in the Oslo rift. In: Norway. *Proceedings, 37th workshop on geothermal reservoir engineering*, Stanford University.
- Ikechukwu, I. O., Derick, C. A. and Olusola, O. B., 2015, Exploration and application of geothermal energy in Nigeria. *International Journal of Scientific and Engineering Research*, 6(2), 726, ISSN 2229-5518.
- Jaupart, C. and Mareschal, J. C., 2003, Constraints on crustal heat production from heat flow data. In: *Treatise of geochemistry: the crust*. Rudnick, Elsevier, (3), 65-84.
- Kasidi, S. and Nur, A. 2012, Curie depth isotherm deduced from spectral analysis of Magnetic data over sarti and environs of North-Eastern Nigeria. *Scholarly Journal of Biotechnology*, 1(3), 49 -56.
- Kasidi, S. and Nur, A., 2013, Estimation of Curie Point depth, heat flow and geothermal gradient inferred from aeromagnetic data over Jalingo and Environs. *International Journal of Science and Emerging Technology*, 6(6), 294-301.
- Kuforijimi, O. and Christopher, A., 2017, Assessment of Aero-radiometric Data of Southern Anambra Basin for the Prospect of Radiogenic Heat Production. *Journal of Applied Science and Environmental Management*. 21(4), 743-748.
- Megwara, J. U., Udensi, E. E., Olasehinde, P. I. Daniyan, M. A. and Lawal, K. M., 2013, Geothermal and radioactive heat studies of parts of southern Bida basin, Nigeria and the surrounding basement rocks. *International Journal of Basic and Applied Sciences*, 2(1), 125-139.
- Mishra, D. C. and Naidu, P. S., 1974, Two Dimensional Power Spectrum and Analysis of Aeromagnetic Fields. *Geophysical Prospecting*, 22(2), 345-353.
- Muffler, P. and Cataldi, R., 1978, Methods for regional assessment of geothermal resources. *Geothermics*, 7, 53-89.
- Nagata, T., 1961, *Rock Magnetism*, 350 pp., Maruzen, Tokyo,
- Nwankwo, L. I., Olasehinde, P. I. and Akaosile, C. O., 2011, Heat flow anomalies from the spectral analysis of airborne magnetic data of Nupe Basin, Nigeria. *Asian Journal of Earth Sciences*, 1(3), 5-6.
- Nwogbo, P. O., 1997, Mapping the shallow magnetic sources in the Upper Benue Basin in Nigeria from aeromagnetic. *Spectra*, 4(3/4), 325-333.

- Nwosu, O. B., 2014, Determination of Magnetic Basement Depth over Parts of Middle Benue Trough by Source Parameter Imaging (SPI) Technique Using HRAM. *International Journal of Scientific & Technology Research*, 3(1), ISSN 2277-8616.
- Obaje, N. G., 1994, Coal Petrology, Microfossils and Palaeoenvironments of Cretaceous Coal Measures in the Middle Benue Trough of Nigeria. *Tubinger Mikropalaontologische Mitteilugen*, 11, 1-150.
- Obaje, N. G., 2009, Geology and Mineral Resources of Nigeria. *Lecture Notes in Earth Sciences*. Eds.: Bhattacharji, S., Neugebauer, H.J., Reitner, J. and Stuwe, K. pub. Springer.
- Offodile, M. E., 1976, The Geology of the Middle Benue Nigeria. *Cretaceous Research, Paleontological Institute: University of Uppsala. Special Publication*, 4, 1-166.
- Offodile, M. E., 1984, The Geology and Tectonics of Awe Brine Field. *Journal of Earth Sciences*, 2, 191-202.
- Ofoegbu, C. O., 1985, A review of the geology of the Benue trough, Nigeria. *Journal African Earth Sciences*, 283-291.
- Ofor, N. P. and Udensi, E. E., 2014, Determination of the heat flow in the Sokoto Basin, Nigeria using spectral analysis of aeromagnetic data. *Journal of Natural Sciences Research*, 83-93.
- Okubo, Y., Graf R. J., Hansen, R. O., Ogawa, K. and Tsu, H., 1985, Curie point depths of the Island of Kyushu and surrounding areas, Japan. *Geophysics*, 53(3), 481-494.
- Okubo, Y., Tsu, H. and Ogawa, K., 1989, Estimation of Curie point temperature and geothermal structure of Island arc of Japan. *Tectonophysics*, 159, 279-290.
- Onuoha, K. M., Ofoegbu, C. O. and Ahmed, M. N., 1994, Spectral Analysis of Aeromagnetic Data over the Middle Benue Trough, Nigeria. *Journal of Mining and Geology*, 30, (2), 211-217.
- Osazuwa, I. B., Ajakaiye, D. E. and Verheijen, P. J. T., 1981, Analysis of the structure of part of the upper Benue rift valley on the basis of new geophysical data. *Earth Evolution Sciences*, 2, 126-135.
- Patrick, N. O., Fadele, S. I. and Adegoke, I., 2013, Stratigraphic report of the middle Benue Trough, Nigeria: Insights from petrographic and structural evaluation of Abuni and Environs part of late Albian-Cenomanian Awe and Keana Formations. *The Pacific Journal of Science and Technology*, 14, 557-570. Retrieved from <http://www.akamaiuniversity.us/PJST.htm>
- Ross, H. E., Blakely, R. J. and Zoback, M. D., 2006, Testing the use of aeromagnetic data for the determination of Curie depth in California. *Geophysics*, 71(5), L51-L59.
- Rybach, L., 1976, Radioactive heat production in rocks and its relation to other Petrophysical parameters. *Pure and Applied Geophysics*, 114, 309-318.
- Sedara, S. O. and Joshua, E. O., 2013, Evaluation of the existing state of geothermal exploration and development in Nigeria. *Journal of Advances in Physics*, 2(2), 118-123, ISSN 2347-3487.
- Salako, K. A. and Udensi, E. E., 2013, Spectral depth analysis of parts of upper Benue Trough and Borno Basin, North-East Nigeria, using aeromagnetic data. *International Journal of Science and Research (IJSR)*, 2(8), 2319-7064.
- Shuey, R. T., Schellinger, D. K., Tripp, A. C. and Alley, L. B., 1977, Curie depth determination from aeromagnetic spectra. *Geophysical Journal Royal Astronomical Society*, 50, 75-101.
- Slagstad, T., 2008, Radiogenic heat production of Archean to Permian geological provinces in Norway. *Norwegian Journal of Geology*, 88, 149-166.
- Spector, A. and Grant, F. S., 1970, Statistical models for interpreting aeromagnetic data. *Geophysics*, 35, 293-302.
- Stacey, F. D., 1977, *Physics of the Earth*. John Wiley and Sons publication New York, NY, USA: 2nd edition.
- Tanaka, A., Okubo, Y. and Matsubayash, O., 1999, Curie point depth based on spectral analysis of the magnetic anomaly data in East and South-East Asia. *Tectonophysics*, 306, 461-470.
- Telford, W. M., Geldart, L. P. and Sherif, R. E., 1990, *Applied Geophysics*. Cambridge: Cambridge University Press.